DTU Library

Two-dimensional Kagome photonic bandgap waveguide

Nielsen, Jens Bo; Søndergaard, Thomas; Libori, Stig E. Barkou; Bjarklev, Anders Overgaard; Broeng, Jes

[Link back to DTU Orbit](#)

Two-Dimensional Kagomé Photonic Bandgap Waveguide

Jens Bo Nielsen, Thomas Søndergaard, Stig E. Barkou, Anders Bjarklev, and Jes Broeng

Abstract—The transverse-magnetic photonic-bandgap-guid- ance properties are investigated for a planar two-dimensional (2-D) Kagomé waveguide configuration using a full-vectorial plane-wave-expansion method. Single-moded well-localized low-index guided modes are found. The localization of the optical modes is investigated with respect to the width of the 2-D Kagomé waveguide, and the number of modes existing for specific frequen- cies and waveguide widths is mapped out.

Index Terms—Integrated optics, Kagomé lattice, periodic struc- tures, photonic bandgap, submillimeter wave waveguides.

I N RECENT YEARS, a new class of periodic dielectric struc- tures, known as photonic bandgap structures, has been dis- covered [1]. These structures are characterized by one or more frequency intervals, photonic bandgaps, where propagation of electromagnetic waves is not allowed. By introducing a prop- erly designed defect in a photonic bandgap structure strong lo- calization of photon waves to the region near the defect is pos- sible. A novel microcavity design may be obtained by intro- ducing a point defect, whereas novel waveguide designs may be obtained by introducing a line defect. A recent theoretical result for a waveguide based on introducing a line defect in a two-dimensional (2-D) photonic bandgap structure showed that a transmission of 98% around a 90° sharp bend is possible [2]. The most commonly known 2-D photonic bandgap structures are the square lattice structure [3], [4], the triangular structure [5], [6], and the Honeycomb structure [7], [8]. It is a technolog- ical challenge to fabricate photonic bandgap structures for op- tical wavelengths, since the lattice constant of the periodic struc- ture must be comparable to the optical wavelength. For struc- tures based on GaAs rods in air, one approach is to use selective epitaxy [9].

In this letter, a waveguide based on a third fundamental hexagonal photonic bandgap structure, known as the Kagomé structure [10], is investigated for the first time. This wave- guide, shown in Fig. 1 along with the coordinate system, consists of a homogeneous layer, the line defect, sandwiched between two semi-infinite layers of the Kagomé structure with circular dielectric rods in air. The parameters defining the 2-D waveguide structure are the background dielectric constant $\varepsilon_{\text{back}} = 1$ (air), the dielectric constant of the rods $\varepsilon_{\text{rod}} = 13$ (representative of GaAs at optical frequencies), the rod diameter D, the center-to-center distance between rods Λ,
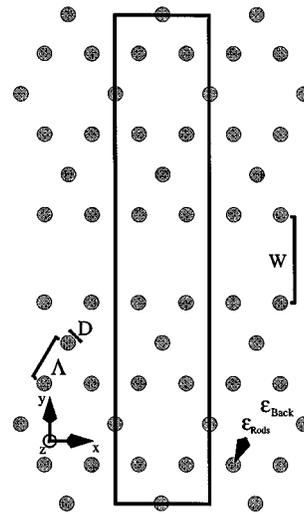
The Kagomé Waveguide

Fig. 1. The structure of the Kagomé waveguide is shown, along with an example of a supercell and the parameters necessary to characterize the structure.
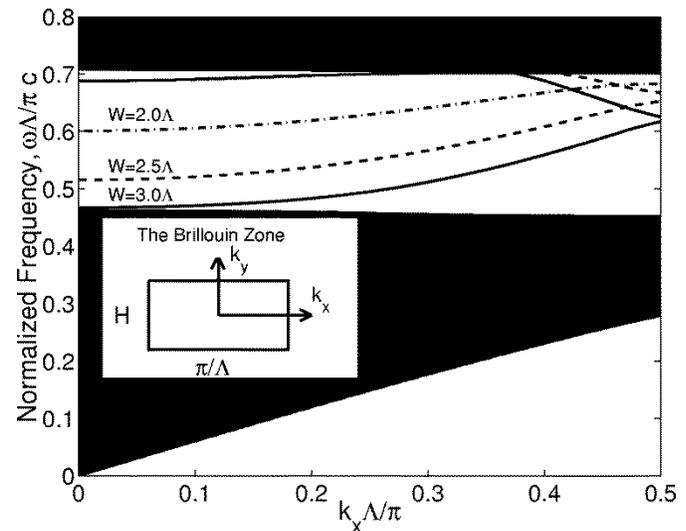
Fig. 2. TM band diagram of the Kagomé waveguide with localized modes for three different waveguide widths.

and the center-to-center waveguide width W. The structure is invariant in the out-of-plane direction (the z-direction).

The results presented in this letter were calculated using a computer model based on the full-vectorial plane-wave-expan- sion method described in [11]. In the calculations the Kagomé waveguide is approximated by a periodic structure using

Fig. 3. The frequency domain of modes for small waveguide widths. Single-moded and dual-moded domains are colored light and dark, respectively. The thin domain edge corresponds to $k_x = 0$, while the thick edge corresponds to $k_x = \pi/2\Lambda$.
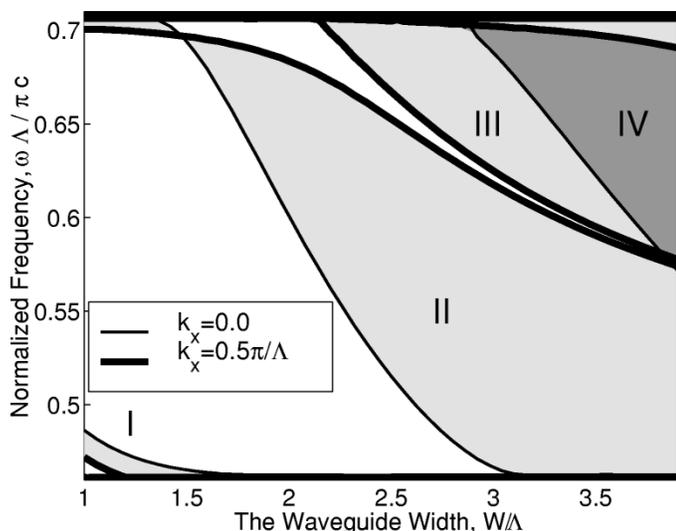

Fig. 4. Six field plots shows the dependency of localization and field structure upon the waveguide width W and the k_x value.

a supercell approximation. An example of a supercell of height $H = W + 5\sqrt{3}\Lambda$ is shown in Fig. 1. In the actual calculations, a supercell of height $H = W + 9\sqrt{3}\Lambda$ was used, except for Fig. 3, where a supercell of height $H = W + 17\sqrt{3}\Lambda$ was used to test the convergence of the calculations. The differences in frequency between the calculations with supercell height $H = W + 9\sqrt{3}\Lambda$ and $H = W + 17\sqrt{3}\Lambda$ were smaller than 0.6%.

For in-plane investigations it is common to categorize the modes in TE and TM modes defined as the modes having their electric and magnetic fields, respectively, in the plane of investigation (the xy-plane). In this letter, we will restrict our attention to TM polarized modes, and therefore choose the rod diameter $D = 0.45\Lambda$ yielding the largest TM photonic bandgap for the Kagomé rod structure with the dielectric constants being 1 for the background and 13 for the rods [9]. For waveguides, taking advantage of a strictly TM photonic bandgap, only TM polarized modes may become guided, and consequently the waveguide will be extremely polarization sensitive (operating as a polarizer). TM bandgap guided modes, being localized to the line defect, are characterized by a frequency within the photonic bandgap of the surrounding photonic crystal. In particular, it is possible to guide light using a line defect with a low concentration of high-index material compared to the surrounding structure, and therefore the guiding mechanism, photonic bandgap guidance, is fundamentally different from conventional index-guiding waveguides. In this letter we consider the concentration of high-index material in the waveguiding region to be high compared to the surrounding structure for waveguide widths W shorter than 1.0Λ. Consequently, only widths larger than 1.0Λ are investigated in this paper.

The band diagram shown in Fig. 2 was obtained from calculations with a supercell height $H = W + 9\sqrt{3}\Lambda$, where the bands on either side of the bandgap are not completely dense. The dense bands shown in Fig. 2 correspond to an infinitely high supercell. In the case of an infinitely high supercell, it is
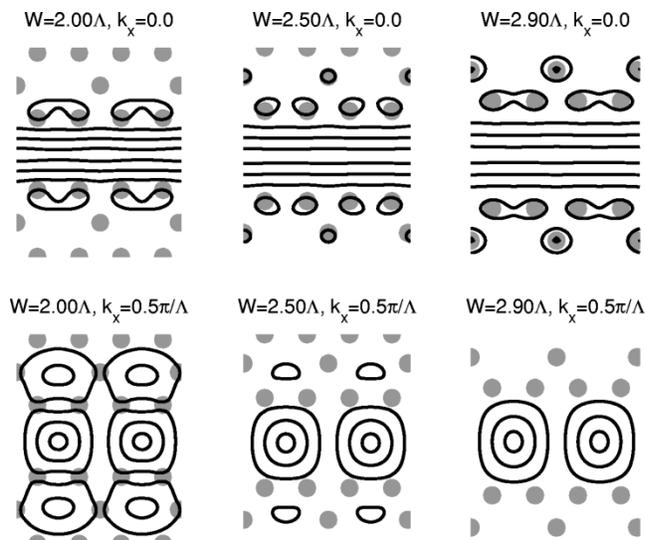
only necessary to probe the bandgap structure along the k_x-axis from zero to $\pi/2\Lambda$, because of the collapse of the irreducible Brillouin zone in the k_y-direction as H tends toward infinity.

The guided modes of three different waveguide widths are shown in the bandgap. The monotone sweep of frequencies between $k_x = 0$ and $k_x = \pi/2\Lambda$ means that only the $k_x = 0$ and $k_x = \pi/2\Lambda$ points in the Brillouin zone need to be calculated in order to obtain the frequency intervals of guided modes for given waveguide widths. Fig. 3 shows these frequency intervals as a function of waveguide width W, where single-moded and dual-moded domains are shaded light and dark, respectively. This is interesting from a construction point of view, as single-moded waveguides are generally more useful than multi-moded waveguides.

With respect to the bandgap edges, Fig. 3 only shows the general picture, as the TM bandgap edges depend slightly upon k_x. The bandgap shown in Fig. 3 is the maximum bandgap valid for the complete set of k_x-values. The thin domain edge corresponds to $k_x = 0$, while the thick edge corresponds to $k_x = \pi/2\Lambda$.

Using Fig. 3, it is possible to determine the characteristic parameters introduced in Fig. 1, if the frequency of the wave in the waveguide is given. Choosing a wavelength of 1550 nm (the standard wavelength of optical communications), a normalized frequency of 0.6, and a waveguide width of 2.2Λ as an example, a single guided mode far from the bandgap edges is obtained. In this example Λ is 465 nm, hence D is 209 nm, and thus the structure appears realizable [9].

Fig. 4 shows six field plots (the electric field amplitude squared) of modes from mode-domain II. It demonstrates that the modes are localized better far from the bandgap edges. This is observed by comparing Figs. 3 and 4: As the waveguide width increases, we know from Fig. 3 that mode-domain II is approaching the bandgap edge in the case of $k_x = 0$. Fig. 4 shows a decreasingly localized mode. The same line of argument applies for $k_x = \pi/2\Lambda$, where modes in larger waveguides are better localized.

Although changes in the waveguide width affect the localization of the modes for a given k_x, the field intensity distribution is almost unaffected until the modes becomes completely delocalized. The transition from a guided to an unguided mode will of course have an effect. With respect to variations in k_x, both the localization (as explained above) and the field structure are affected simultaneously. The field structures shown in Fig. 4 are clearly different for $k_x = 0$ and $k_x = \pi/2\Lambda$. In fact, the field structure transforms continuously from one to the other as k_x goes from $k_x = 0$ to $k_x = \pi/2\Lambda$.

In conclusion, we have theoretically investigated a waveguide consisting of a line defect within a new fundamental hexagonal photonic bandgap material, the Kagomé structure. The investigation shows the Kagomé waveguide to have well-localized low-index-guided TM modes, and that the TM modes are better localized far from the bandgap edges. Furthermore, the frequency domain of the TM guided modes for small waveguide widths have been mapped out, allowing us to determine the number of guided modes in the waveguide for specific waveguide widths and frequencies.

REFERENCES

[1] E. Yablonovitch, "Photonic band-gap structures," *J. Opt. Soc. Amer. B.*, vol. 10, no. 2, pp. 283–295, 1993.
[2] A. Mekis, J. C. Chen, I. Kurland, S. Fan, P. R. Villeneuve, and J. D. Joannopoulos, "High transmission through sharp bends in photonic crystal waveguides," *Phys. Rev. Lett.*, vol. 77, no. 18, pp. 3787–3790, 1996.
[3] A. Mekis, S. Fan, and J. D. Joannopoulos, "Bound states in photonic crystal waveguides and waveguide bends," *Phys. Rev. B.*, vol. 58, no. 8, pp. 4809–4817, 1998.
[4] J. D. Joannopoulos, R. D. Meade, and J. N. Winn, *Photonic Crystals, Molding the Flow of Light*. Princeton, NJ: Princeton Univ. Press, 1995.
[5] H. Benisty, "Modal analysis of optical guides with two-dimensional photonic band-gap boundaries," *J. Appl. Phys.*, vol. 79, no. 10, pp. 7483–7492, 1996.
[6] M. Plihal and A. A. Maradudin, "Photonic band structures of two-dimensional systems: The triangular lattice," *Phys. Rev. B.*, vol. 44, no. 16, pp. 8565–8571, 1991.
[7] T. Søndergaard, J. Broeng, A. Bjarklev, K. Didri, and S. E. Barkou, "Suppression of spontaneous emission for a two-dimensional honeycomb photonic bandgap structure estimated using a new effective-index model," *IEEE J. Quantum Electron.*, vol. 34, no. 12, pp. 2308–2313, 1998.
[8] D. Cassagne, C. Jouanin, and D. Bertho, "Photonic band gaps in a two-dimensional graphite structure," *Phys. Rev. B.*, vol. 52, no. 4, pp. R2217–R2220, 1995.
[9] T. Hamano, H. Hirayama, and Y. Aoyagi, "New technique for fabrication of two-dimensional photonic bandgap crystals by selective epitaxy," *J. Appl. Phys.*, vol. 36, pp. L286–L288, 1997.
[10] J. B. Nielsen, T. Søndergaard, S. E. Barkou, A. Bjarklev, J. Broeng, and M. B. Nielsen, "The two-dimensional Kagomé structure, a new fundamental hexagonal photonic crystal configuration," *Electron. Lett.*, vol. 35, no. 20, pp. 1736–1737, 1999.
[11] R. D. Meade, A. M. Rappe, K. D. Brommer, J. D. Joannopoulos, and O. L. Alerhand, "Accurate theoretical analysis of photonic band-gap materials," *Phys. Rev. B.*, vol. 48, pp. 8434–8437, 1993.